

Supporting Information

Keplinger et al. 10.1073/pnas.0913461107

SI Text

Experimental Details. Fig. S1 (*Left*) illustrates the Kelvin probe measurement to obtain the surface potential of the elastomer. The vertical gray stripe depicts the cross section of the elastomer. The blue and yellow squares illustrate the sprayed-on charges, and the electric field is illustrated by small arrows. In addition, equipotential lines are drawn. To assess the surface potential of the elastomer via non-contact measurements, the housing of the probe head (gray rectangle with yellow border) is driven to a potential equal to the surface potential of the elastomer by approximately nulling the electric field in the gap. Fig. S1 (*Right*) shows the experimental arrangement with two Kelvin probes to measure the potentials $\varphi_{1,2}$ on both surfaces of the elastomer; the voltage U between the two elastomer surfaces is then obtained from the potential difference between the two Kelvin probe readings.

In Fig. 3 it seems surprising that the voltage measured at the highest stretch ratio of 1.25 is smaller than the voltage at the lower stretch ratio of 1.15, although there are more charges on the elastomer at a stretch ratio of 1.25 as compared to the stretch ratio of 1.15. Fig. S2 illustrates such a situation. Whereas on the left side, with a thick elastomer the charge Q_1 is smaller than the charge Q_2 , on the right side, with a thinner elastomer and a larger area, the opposite is true for the voltages: U_1 is larger than U_2 .

The geometry for the theoretical modeling is illustrated in Fig. S3. The initial dimensions of the elastomer are denoted with a subscript i ; the dimensions p stand for the prestretched state. The transition from the i to the p state is partly viscoelastic. The reference state 0 can be obtained on a short time scale if the mass m used for prestretching is removed. Stretching to the final state after charging is described from the reference state 0.

Fig. S4 illustrates the excellent fit used to obtain the prestretch parameter $\lambda_{px} = 1.42$, as discussed in the main text.

Experiments shown in Figs. 4 and 5 of the manuscript are illustrated with two video files. In Movie S1 the reversibility of the large deformations of an elastomer surface is demonstrated. Even the huge irregular deformations visible in Fig. 4D fully recover to the initial flat state.

Movie S2 illustrates the operation of the electrode-free bending actuator. The speed of operation is currently limited by the used dc high-voltage power supply. In order to discharge the actuator, the polarity of the supply must be changed. This is only possible by switching the device off, followed by a manual change of polarity.

Theoretical Considerations on Elastomer Stripes with Sprayed-on Charges. An elastomer with sprayed-on electrical charges differs significantly from a deformable electrode coated capacitor. Conducting electrodes are equipotential surfaces, and the free flow of electrons along them concentrates the charges near the edges and corners of the structure. In contrast, elastomers with sprayed-on electrical charges may have charge distributions that are different on the top and bottom surface of the elastomer. In the article we have made the approximation that the energetics of an elastomer with sprayed-on electrical charges is dominated by the usual capacitor term.

In order to verify our approximations, we rigorously solve the problem of a plane dielectric of finite thickness h with arbitrary surface charge densities on both sides. The electrostatic energy can be written in two equivalent forms (1) (centimeter-gram-second Gaussian system is used here): $W = \frac{1}{8\pi} \int \mathbf{E} \mathbf{D} dV =$

$\frac{1}{2} \int \varphi dq$. The last integral can be over the volume, or surface, or a mixture of both. It is usually simpler than the first expression, especially when the integration should be done only over the surface charges as in our case. To calculate the energy, we solve a Poisson-type equation for the potential φ , $\text{div} \mathbf{D} = -\text{div}(\epsilon \text{grad} \varphi) = 4\pi\rho$ everywhere; find the field $\mathbf{E} = -\nabla\varphi$ and the displacement $\mathbf{D} = \epsilon\mathbf{E}$ and calculate the energy using any of the two aforementioned integrals.

The dielectric will occupy a layer $0 < z < h$, and subscripts 0 and h refer to the corresponding z planes. Subscript e refers to the elastomer. Because only surface charge densities σ are present, the potential satisfies the Laplace equation $\Delta_{\perp}\varphi + \varphi_{zz} = 0$ both inside and outside of the elastomer. Here we mean under Δ_{\perp} the part of the Laplacian in the (x,y) plane $\Delta_{\perp} = \partial_{xx} + \partial_{yy}$. Applying a Fourier transformation in the x - y plane (denoted by tilde, $\tilde{\varphi}$) we get $-k^2\tilde{\varphi} + \tilde{\varphi}_{zz} = 0$ where $k^2 = k_x^2 + k_y^2$ is the square of the Fourier wavevector, and the subscript z denotes differentiation. The solutions of this equation outside and inside the elastomer can be written as

$$\begin{aligned} \tilde{\varphi}_{-} &= c_{-}e^{kz}, & z < 0; & & \tilde{\varphi}_{e} &= c_1e^{kz} + c_2e^{-kz}, & 0 < z < h; \\ \tilde{\varphi}_{+} &= c_{+}e^{-k(z-h)}, & z > h. & & & & \end{aligned} \quad [\text{S1}]$$

With such notations the conditions at infinities are satisfied automatically, and the coefficients c_{\pm} have the meaning of the potentials on both surfaces: $\tilde{\varphi}_0 = c_{-}$, $\tilde{\varphi}_h = c_{+}$. The continuity of the potential and the change in the normal derivative of (Fourier image of) the electric displacement $\tilde{D}_n \equiv (1 \text{ or } \epsilon)\tilde{E}_n \equiv -(1 \text{ or } \epsilon)\tilde{\varphi}_z$ on both surfaces can be written as follows:

$$\begin{aligned} \tilde{\varphi}_{-}(0) &= \tilde{\varphi}_e(0) \Rightarrow c_{-} = c_1 + c_2, \\ \epsilon \frac{d\tilde{\varphi}_e}{dz} \Big|_0 - \frac{d\tilde{\varphi}_{-}}{dz} \Big|_0 + 4\pi\tilde{\sigma}_0 &= 0 \Rightarrow kc_{-} - \epsilon k(c_1 - c_2) = 4\pi\tilde{\sigma}_0, \\ \tilde{\varphi}_{+}(h) &= \tilde{\varphi}_e(h) \Rightarrow c_{+} = c_1e^{kh} + c_2e^{-kh}, \\ \frac{d\tilde{\varphi}_{+}}{dz} \Big|_h - \epsilon \frac{d\tilde{\varphi}_e}{dz} \Big|_h + 4\pi\tilde{\sigma}_h &= 0 \Rightarrow kc_{+} + \epsilon k(c_1e^{kh} - c_2e^{-kh}) = 4\pi\tilde{\sigma}_h. \end{aligned} \quad [\text{S2}]$$

This system of linear equations can be easily solved. Subsequently, we will often use symmetric and asymmetric parts of the charge and potential distributions (or their Fourier transforms), defined as follows:

$$\begin{aligned} \sigma &= \sigma_h + \sigma_0, & \delta &= \sigma_h - \sigma_0, & \text{which implies } \sigma_{0,h} &= (\sigma \mp \delta)/2 \\ u &= \varphi_h + \varphi_0, & v &= \varphi_h - \varphi_0, & \varphi_{0,h} &= (u \mp v)/2. \end{aligned} \quad [\text{S3}]$$

With these notations, the coefficients c_{\pm} , which are equal to the surface potentials, are found to be

$$c_{\mp} \equiv \tilde{\varphi}_{0,h} = \frac{2\pi}{k} \left(\frac{\tilde{\sigma}}{1 + \epsilon \text{th} \frac{kh}{2}} \mp \frac{\delta \text{th} \frac{kh}{2}}{\epsilon + \text{th} \frac{kh}{2}} \right). \quad [\text{S4}]$$

We use these formulas to relate charge densities and potentials. Their symmetric and asymmetric parts separate and are proportional to each other in Fourier space:

$$\begin{aligned}
\tilde{\sigma} &= \frac{k}{4\pi} \left(1 + \varepsilon \text{th} \frac{kh}{2} \right) \tilde{u} \approx \frac{k}{4\pi} \tilde{u} + \underbrace{O(h^2 k \tilde{u})}_{\leq h^2 k \tilde{v}}, \\
\tilde{\delta} &= \frac{k}{4\pi} \frac{\varepsilon + \text{th} \frac{kh}{2}}{\text{th} \frac{kh}{2}} \tilde{v} \approx \left(\frac{\varepsilon}{2\pi h} + \frac{k}{4\pi} \right) \tilde{v} + \underbrace{O(h^2 k \tilde{v})}_{\sim h^2 k \tilde{v}}, \\
\tilde{u} &= \frac{4\pi}{k} \frac{\tilde{\sigma}}{1 + \varepsilon \text{th} \frac{kh}{2}} \approx \frac{4\pi}{k} \tilde{\sigma} + \underbrace{O(h \tilde{\sigma})}_{\sim h k \tilde{u} \leq h k \tilde{v}}, \\
\tilde{v} &= \frac{4\pi}{k} \frac{\tilde{\delta} \text{th} \frac{kh}{2}}{\varepsilon + \text{th} \frac{kh}{2}} \approx \left(\frac{2\pi h}{\varepsilon} - \frac{\pi h^2 k}{\varepsilon^2} \right) \tilde{\delta} + \underbrace{O(h^3 k^2 \tilde{\delta})}_{\sim h^2 k^2 \tilde{v}}.
\end{aligned} \tag{S5}$$

The approximate expressions are Taylor expansions up to the first meaningful order in (small) thickness h . It requires a different number of terms in different formulas, as will become clear from the energy expressions below. There exists subtlety in the comparison between the different terms in the potential and charge representation. If the characteristic in-plane size of the system is a , the important wavevectors are $k \sim 1/a$, and the small parameter in the Taylor expansion is $hk \sim h/a \ll 1$. From the Fourier representation (Eq. S5) we get

$$\frac{\tilde{\sigma}}{\tilde{\delta}} = \frac{1 + \varepsilon \text{th} \frac{kh}{2}}{\frac{\varepsilon + \text{th} \frac{kh}{2}}{\text{th} \frac{kh}{2}}} \frac{\tilde{u}}{\tilde{v}} \approx \frac{kh \tilde{u}}{2\varepsilon \tilde{v}}. \tag{S6}$$

This means that the ratio of the symmetric/asymmetric terms always has a different order of magnitude for charges and potentials. For our experimental conditions it is always small for the charges, but not necessarily small for the potentials. From the experiment, we know that typically $u \leq v$. Correspondingly, $\sigma \leq kh\delta \ll \delta$. As shown below, the symmetric and asymmetric parts separate in the energy expression in the Fourier space (Eq. S13). The coefficient in the asymmetric potential term is a factor of $1/kh$ larger than for the symmetric part. For this reason we make a Taylor expansion up to zero order in the symmetric terms, but up to the first order in asymmetric ones. Orders of magnitude of the errors for the worst realistic case $u \sim v$ are indicated in Eq. S5.

The approximate formulas for small thicknesses can be analytically Fourier-inverted for arbitrary charge densities. The two-dimensional (2D) (direct or inverse) Fourier transform (with symmetric prefactor) has the following properties (2):

$$\tilde{k}^{-1} = r^{-1}, \quad f^* \tilde{g} = 2\pi \tilde{f} \tilde{g}, \quad \Delta_{\perp} f = -k^2 \tilde{f}. \tag{S7}$$

Here the asterisks stands for 2D convolution. The inversion of \tilde{k} cannot be done in a similar fashion because of the singularities involved. Using the first two properties, we can obtain a Fourier inversion of the expression

$$\tilde{\varphi}_s = \frac{2\pi}{k} \tilde{\sigma}, \quad \text{which is the single-layer potential} \quad \varphi_s \equiv \sigma * \frac{1}{r}. \tag{S8}$$

The Fourier inversion of the function f in combination with different powers of k can be written as follows:

$$\begin{aligned}
\frac{1}{k} \tilde{\tilde{f}} &= \frac{1}{2\pi r} * f, & \tilde{\tilde{f}} &= f, & k \tilde{\tilde{f}} &= \frac{-1}{k} (\tilde{-k^2 \tilde{f}}) = \frac{-1}{2\pi r} * \Delta_{\perp} f, \\
k^2 \tilde{\tilde{f}} &= -\Delta_{\perp} f.
\end{aligned} \tag{S9}$$

This allows us to invert analytically the small thickness expressions in Eq. S5:

$$\begin{aligned}
\sigma &\approx -\frac{1}{8\pi^2 r} * \Delta_{\perp} u, & \delta &\approx \frac{\varepsilon}{2\pi h} v - \frac{1}{8\pi^2 r} * \Delta_{\perp} v, & u &\approx \frac{2}{r} * \sigma, \\
v &\approx \frac{2\pi h}{\varepsilon} \delta + \frac{h^2}{2\varepsilon^2 r} * \Delta_{\perp} \delta.
\end{aligned} \tag{S10}$$

For the surface potentials in terms of charge densities and vice versa we get

$$\begin{aligned}
\varphi_{0,h} &= \frac{u \mp v}{2} \approx \underbrace{\frac{1}{r} * \sigma}_{\varphi_s} \mp \left(\frac{\pi h}{\varepsilon} \delta + \frac{h^2}{4\varepsilon^2 r} * \Delta_{\perp} \delta \right), \\
\sigma_{0,h} &= \frac{\sigma \mp \delta}{2} \approx -\frac{1}{16\pi^2 r} * \Delta_{\perp} u \mp \left(\frac{\varepsilon}{4\pi h} v - \frac{1}{16\pi^2 r} * \Delta_{\perp} v \right) \\
&= -\frac{1}{16\pi^2 r} * \Delta_{\perp} \varphi(0, h) \mp \frac{\varepsilon}{4\pi h} v.
\end{aligned} \tag{S11}$$

One can recognize the global potential of the single layer φ_s , the double layer capacitor term, and some addition related to the in-plane inhomogeneity of the double layer in the simplified expressions. Surface charge densities in terms of potentials are given by the contributions from the global term for each surface potential and the asymmetric capacitor contribution.

Total electrostatic energy. It is convenient to calculate the energy in the Fourier space, because then the intermediate results are exact. According to Parseval's theorem (2) (in unitary convention), $\iint f g^* dS = \iint \tilde{f} \tilde{g}^* dS_k$. Here asterisk superscripts denote complex conjugates. Thus, the energy can also be calculated as the integral of the product of the Fourier images of the charges and potentials. All our functions are real and even with respect to x and y (or can be made even by quadrupling of their domain). Therefore, their Fourier transforms are also real, and we can write for the surface differential of the electrostatic energy:

$$\begin{aligned}
dW &= \frac{\varphi_0 \sigma_0 + \varphi_h \sigma_h}{2} dS = \frac{u\sigma + v\delta}{4} dS \rightarrow \frac{\tilde{\varphi}_0 \tilde{\sigma}_0 + \tilde{\varphi}_h \tilde{\sigma}_h}{2} dS_k \\
&= \frac{\tilde{u} \tilde{\sigma} + \tilde{v} \tilde{\delta}}{4} dS_k.
\end{aligned} \tag{S12}$$

Using the relationships in Eq. S5, this can be written in terms of charges or potentials only, in exact or in approximate form. Symmetric and asymmetric variables $u \propto \sigma$, $v \propto \delta$ separate, and the energy is always diagonal in terms of these variables:

$$\begin{aligned}
dW &= \frac{k}{16\pi} \left(\left(1 + \varepsilon \text{th} \frac{kh}{2} \right) \tilde{u}^2 + \frac{\varepsilon + \text{th} \frac{kh}{2}}{\text{th} \frac{kh}{2}} \tilde{v}^2 \right) dS_k \\
&= \frac{\pi}{k} \left(\frac{\tilde{\sigma}^2}{1 + \varepsilon \text{th} \frac{kh}{2}} + \frac{\tilde{\delta}^2 \text{th} \frac{kh}{2}}{\varepsilon + \text{th} \frac{kh}{2}} \right) dS_k \\
&\approx \left(\underbrace{\frac{k \tilde{u}^2}{16\pi}}_{\leq k v^2} + \underbrace{\frac{\varepsilon \tilde{v}^2}{8\pi h}}_{\substack{(kh)^{-1} k v^2 \\ \gg k v^2}} + \underbrace{\frac{k \tilde{v}^2}{16\pi}}_{k v^2} \right) dS_k \\
&\approx \left(\underbrace{\frac{\pi \tilde{\sigma}^2}{k}}_{\substack{\leq (kh)^2 \sigma^2 / k \\ \leq (kh) h \delta^2}} + \underbrace{\frac{\pi h \tilde{\delta}^2}{2\varepsilon}}_{\substack{h \delta^2 \\ \gg (kh) h \delta^2}} - \underbrace{\frac{\pi h^2 k \tilde{\delta}^2}{4\varepsilon^2}}_{(kh) h \delta^2} \right) dS_k.
\end{aligned} \tag{S13}$$

Under each term of the Taylor expansion, we indicated the relation to the last term (lowest order correction in v and δ), assuming the worst case $u \sim v$. For $u \ll v$ the terms with u or σ

should be dropped, because omitted terms with v and δ are larger. But we always retain the leading correction in v and δ . The central (capacitor) term is the largest unless $u \gg v$ (almost equal charges on both sides). In this case not all terms in Eq. S13 are meaningful, but the largest term is related to the u or σ expressions (global energy of a single layer). The transition to this regime occurs with $u^2 \sim v^2 a/h$.

Let us transform the approximate energy expression in Eq. S13 written in terms of potentials using the approximate potential-charge relations from Eq. S5. If we retain only the leading terms after squaring, this results in

$$\begin{aligned}
 dW &\approx \left(\underbrace{\frac{k\tilde{u}^2}{16\pi}}_{\leq kv^2} + \underbrace{\frac{\varepsilon\tilde{v}^2}{8\pi h}}_{\substack{(kh)^{-1}k^2 \\ \gg kv^2}} + \underbrace{\frac{k\tilde{v}^2}{16\pi}}_{kv^2} \right) dS_k \\
 &\approx \left(\underbrace{\frac{\pi\tilde{\sigma}^2}{k}}_{\substack{\leq (kh)^2\tilde{\sigma}^2/k \\ \leq (kh)h\delta^2}} + \underbrace{\frac{\pi h\tilde{\delta}^2}{2\varepsilon}}_{\substack{h\delta^2 \\ \gg (kh)h\delta^2}} - \underbrace{\frac{\pi h^2 k\tilde{\delta}^2}{2\varepsilon^2}}_{(kh)h\delta^2} + \underbrace{\frac{\pi h^2 k\tilde{\delta}^2}{4\varepsilon^2}}_{(kh)h\delta^2} \right) dS_k \\
 &\approx \left(\underbrace{\frac{\pi\tilde{\sigma}^2}{k}}_{\substack{\leq (kh)^2\tilde{\sigma}^2/k \\ \leq (kh)h\delta^2}} + \underbrace{\frac{\pi h\tilde{\delta}^2}{2\varepsilon}}_{\substack{h\delta^2 \\ \gg (kh)h\delta^2}} - \underbrace{\frac{\pi h^2 k\tilde{\delta}^2}{4\varepsilon^2}}_{(kh)h\delta^2} \right) dS_k. \quad [\text{S14}]
 \end{aligned}$$

Therefore, we recover the last expression (Eq. S13) obtained by Taylor expansion of the energy in the charge representation. The global u term related to the single layer potential always transforms directly into the global σ term and vice versa. The global δ term related to the asymmetric charge distribution contains the contribution from the capacitor v term. Conversely, in the transformation from the charge to the potential representation, the capacitor δ term will contribute to both capacitor v and global v terms.

The inversion of the approximate expressions in Eq. S13 can be performed analytically for arbitrary potentials or charge profiles using Parseval's theorem and properties of the Fourier inversion (Eq. S9). We write the capacitor term in front and indicate the order of magnitude of all terms assuming that typical sizes of the elastomer rectangle are a (smaller side) and b (larger side). Remember that $\sigma \sim kh\delta \sim h\delta/a$, and the convolution brings an area integration factor $\sim ab$:

$$\begin{aligned}
 dW &\approx \left(\frac{\varepsilon\tilde{v}^2}{8\pi h} + \frac{(k\tilde{u})\tilde{u} + (k\tilde{v})\tilde{v}}{16\pi} \right) dS_k \\
 &\rightarrow \left(\frac{\varepsilon v^2}{8\pi h} - \underbrace{\frac{(\frac{1}{r} * \Delta_{\perp} u)u + (\frac{1}{r} * \Delta_{\perp} v)v}{32\pi^2}}_{\substack{v^2/h \\ (ab/b)(u^2/a^2) \leq v^2/a \\ v^2/a}} \right) dS_k \\
 dW &\approx \left(\frac{\pi h\tilde{\delta}^2}{2\varepsilon} + \frac{2\pi\tilde{\sigma}^2}{k} - \frac{\pi h^2(k\tilde{\delta})\tilde{\delta}}{4\varepsilon^2} \right) dS_k \quad [\text{S15}] \\
 &\rightarrow \left(\frac{\pi\delta^2 h}{2\varepsilon} + \underbrace{\frac{(\frac{1}{r} * \sigma)\sigma}{2}}_{\substack{\varphi\sigma \\ (ab/b)\sigma^2 \leq \delta^2 h^2/a}} + \underbrace{\frac{h^2(\frac{1}{r} * \Delta_{\perp} \delta)\delta}{8\varepsilon^2}}_{h^2(ab/b)(\delta^2/a^2) \sim \delta^2 h^2/a} \right) dS_k.
 \end{aligned}$$

The first term everywhere is the capacitor term. The second term is the global term. As explained above, when one switches between the charge and potential representations, the terms transform into each other in a nontrivial way. Omitted terms

are smaller than at least one of the retained terms. These expressions are not trivial. They involve the integration over the elastomer area and include convolutions and Laplacians. However, orders of magnitude indicated for each term show that for a thin elastomer with $h/a \ll 1$ we can restrict ourselves to the capacitor terms in Eqs. 3 or 5 employed in the main text. Note that there, for practical convenience, we use the International System of Units and the conventional notation U for the asymmetric part of the potential (voltage) v , as defined in Eq. S3.

Although the capacitor term looks deceptively simple, its spatial inhomogeneity accounts for one more subtle and important effect. In plane DEAs with conducting equipotential electrodes, there are no lateral electrostatic forces acting on the elastomer, whereas for nonconducting elastomers with fixed charges they are present and should be reflected in the electrostatic energy. The obtained formulas show that within the approximations made, such forces are taken into account simply by the capacitive energy expression with a variable voltage. Indeed, the potential varies along the surface exactly because the charge distribution is different from that on the equipotential plates of conventional capacitors. The charge distribution might be rather homogeneous in the beginning of the corona spraying cycle. This creates an elevated potential in the center, which deflects subsequently arriving ions toward the edge of the stripe as the charging proceeds. As a result, the final charge density is higher toward the edges, but is not as high as for conducting electrodes. The elevated potential (and voltage) in the middle of the stripe were indeed measured experimentally.

Additional Historical Information. For the interested reader we have copied a few pivotal parts of Quincke's and Röntgen's work in the original German version together with translations in English. In the translation we have tried to keep the initial intent and stylistic flavor of the authors.

Translation of extracts from Quincke's work titled "On electrical expansion" (original German version compiled in Fig. S5) (3):

One will learn from this that solid and liquid isolators change their volume, if they are, similarly to the glass of a Leyden jar, exposed to electrical forces. The volume can increase thereby, what is the most typical, but it can also decrease. The volume change does not originate from electrical compression. The expansion of the glass caused by the electrical forces is homogeneous in all directions, like a thermal expansion, but it does not originate from warming. Simultaneously with the dimensions, also the elastic force of the isolator changes under the influence of the electrical forces. One set of substances shows a decrease here, another set shows an increase.

Thermometer capacitors made of caoutchouc were fabricated in such a way, that in one end of a long, black caoutchouc hose a capillary tube with a fused-in platinum wire was cemented with Shellac and Canada balsam, whereas in the other end a short tube of flint glass was drawn to a needle and similarly fixed.

From these experiments one can learn that the volume increase of caoutchouc is, like it is true for glass and glimmer, almost proportional to the square of the electric potential difference between the capacitor electrodes. Under equal conditions the increase for fresh caoutchouc is ten times higher than for glass; for caoutchouc, which was in contact with water for two days, values are similar to glass.

Translation of extracts from Röntgen's work titled "On the shape- and volume changes of dielectric bodies caused by electricity" (original German version compiled in Fig. S6) (4):

Finally, to those colleagues, who may wish to see an electrical deformation of a solid body without attempting to quantify the process, I would like to recommend the following experiment, which I carried out in 1876, and which I on occasion presented to the assembly of natural scientists in Baden-Baden (1879) among other findings. An approximately 16 cm wide and 100 cm long, rectangular stripe of thin, red caoutchouc is clamped between two small wooden ledges at the top and the bottom; the upper clamp is attached to some kind of arm or hook in such a way, that the caoutchouc stripe hangs freely; the bottom clamp is loaded with weights, which stretch the stripe approximately to the double length. After having waited till the elastic aftereffect has become imperceptible, one observes the position of the bottom end of the stripe, for example on a paper scale placed nearby, while the caoutchouc is electrified by an assistant. For that purpose the assistant holds in each hand an isolated comb of needles, where one of them is connected by a conductor to the positive and the other to the negative electrode of a strong Holtz influence machine; the caoutchouc stripe

hangs between the parallel held combs, but the former is not touched by the needles. As the assistant starts for example at the top and gradually lowers both combs, a larger and larger part of the caoutchouc becomes electrified; accordingly one observes a continuous increase of the length of the band, which finally, when the whole stripe is electrified, amounts to several centimeters. Since dry caoutchouc is a good isolator, this lengthening persists for a long time afterward. It can, however, at least to a large degree, be removed by discharging the stripe, which is done in a similar way to the charging process; but the combs have to be now connected to the ground. Mr. Quincke has also published (1880) similar experiments and believes that one is allowed to conclude from them, that the elasticity of solid bodies is changed by electrical forces; I, from my side, regard this conclusion as rather daring, and after an assessment of Quincke's experiments I didn't find an inducement to share his opinion; however, since I am worried that this article would get too long, I prefer to refrain from disclosing the motives for my negatory attitude.

1. Landau LD, Lifshitz EM, Pitaevskii LP (1984) *Electrodynamics of Continuous Media* (Pergamon, New York), 2nd Ed., *Course of Theoretical Physics*, Vol. 8.
2. Korn GA, Korn TM (2000) *Mathematical Handbook for Scientists and Engineers: Definitions, Theorems, and Formulas for Reference and Review* (Dover, New York), 2nd Ed.
3. Quincke G (1880) Ueber electrische Ausdehnung. *Ann Phys Chem* 10:163–203, 374–414, 513–553.
4. Röntgen WC (1880) Ueber die durch Electricität bewirkten Form—und Volumenänderungen von dielectricischen Körpern. *Ann Phys Chem* 11:771–786.

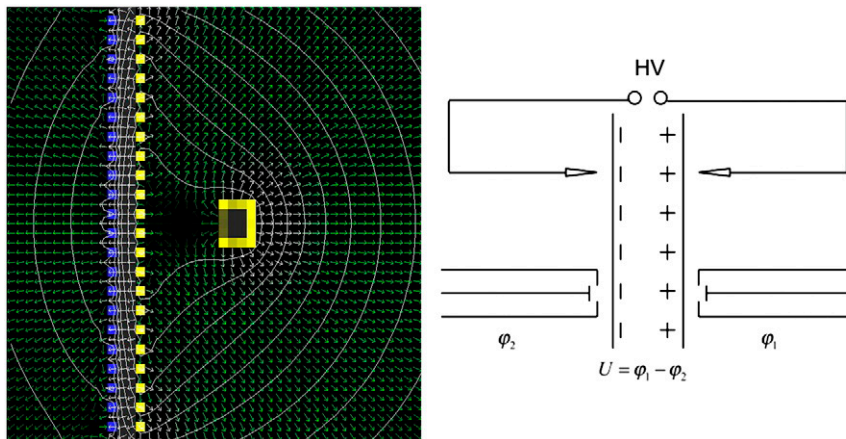


Fig. S1. (Left) Illustration of the Kelvin probe technique for measuring the surface potential. In the Röntgen experiment two Kelvin probes are used to monitor the surface potential on both sides of the film. (Right): Scheme of the experimental setup with two Kelvin probes for measuring the potential on both surfaces of the elastomer.

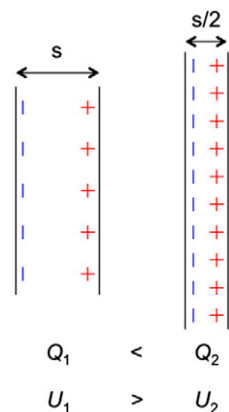


Fig. S2. Schematic illustration of the charges on the elastomer and of the voltages across the elastomer in a thick state with a low stretch ratio and in a thin state with a high stretch ratio, which also has larger area. Whereas the *Left* state can be stable under voltage-controlled conditions, the *Right* state is in the pull-in region. In the charge-controlled operation mode, both states are thermodynamically stable.

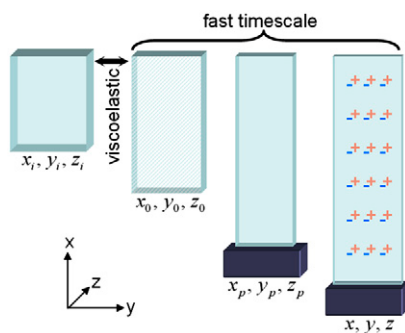


Fig. S3. Illustration of the different deformation dimensions used in the text. The initial state i is characterized by the dimensions x_i, y_i , and z_i , and the weight-loaded state p has sizes x_p, y_p , and z_p . The transition from the i to p state takes several hours and is partly viscoelastic. State 0 with dimensions x_0, y_0 , and z_0 is an auxiliary starting state, which discards viscoelastic effects. The prestretches $\lambda_{px,py,pz}$ characterize the transition from 0 to p . The charged state has the dimensions x, y , and z and is characterized by the secondary stretches $\lambda_{sx,sy,sz}$ referred to the p state.

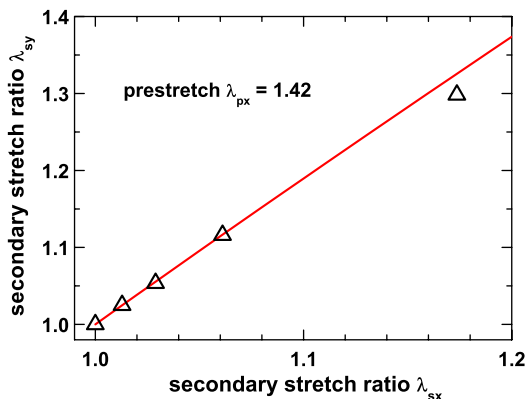


Fig. S4. Relation between the lateral secondary stretches λ_{sy} and λ_{sx} . It allows one to deduce real nonviscoelastic prestretch λ_{px} experimentally. The solid curve, fit with the first equation of Eq. 8, uses a prestretch value of $\lambda_{px} = 1.42$.

Man wird daraus ersehen, dass feste und flüssige Isolatoren ihr Volumen ändern, wenn man sie, ähnlich wie das Glas einer Leydener Flasche, electricischen Kräften aussetzt.

Das Volumen kann dabei vermehrt werden, was das gewöhnlichste ist, oder auch vermindert werden. Die Volumenänderung rührt nicht von electricischer Compression her.

Die von electricischen Kräften hervorgerufene Ausdehnung des Glases erfolgt nach allen Richtungen gleichmässig, wie durch Erwärmung, rührt aber nicht von Erwärmung her.

Gleichzeitig mit den Dimensionen ändert sich auch die elastische Kraft des Isolators unter dem Einflusse der electricischen Kräfte. Bei einer Reihe Substanzen nimmt sie dadurch ab, bei einer andern Reihe zu.

§ 13. Thermometercondensatoren aus Kautschuk wurden in der Weise hergestellt, dass in dem einen Ende eines langen, schwarzen Kautschukschlauchs eine Capillarröhre mit eingeschmolzenem Platindraht, in dem andern Ende ein kurzes, in eine Spitze ausgezogenes Flintglasrohr mit Schellack und Canadabalsam eingekittet wurde.

Aus diesen Versuchen geht hervor, dass die Volumenzunahme des Kautschuks wie bei Glas und Glimmer nahezu proportional ist dem Quadrate der electricischen Potentialdifferenz auf beiden Belegungen des Condensators. Bei sonst gleichen Umständen ist die Zunahme für frischen Kautschuk mehr als zehnmal grösser als bei Glas; für Kautschuk, der zwei Tage mit Wasser in Berührung gewesen, etwa ebenso gross wie bei Glas.

Fig. 55. Extracts from Quincke's original work in German.

Zum Schluss möchte ich denjenigen Fachgenossen, welche vielleicht eine electricische Deformation eines festen Körpers zu sehen wünschen, ohne dieselbe messend verfolgen zu wollen, folgenden Versuch empfehlen, den ich im Jahr 1876 angestellt und bei Gelegenheit der Naturforscherversammlung zu Baden-Baden (1879) unter anderen mitgetheilt habe.¹⁾ Ein ungefähr 16 cm breiter und 100 cm langer, rechteckiger Streifen aus

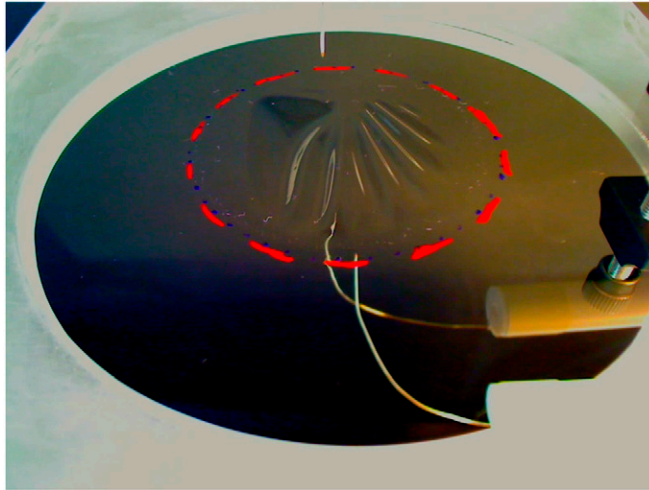
1) Röntgen, Tageblatt der 52. Versammlung, p. 184 1879.
Ann. d. Phys. u. Chem. N. F. XI.

dünnem, rothem Kautschuk wird oben und unten zwischen je zwei Holzleistchen festgeklemmt; die obere Klemme wird an irgend einem Arm oder Haken so befestigt, dass das Kautschukband frei herunterhängt; an die untere Klemme werden Gewichte gehängt, welche den Streifen ungefähr auf die doppelte Länge ausdehnen. Nachdem man gewartet hat, bis die elastische Nachwirkung unmerklich geworden ist, beobachtet man den Stand des untern Endes des Streifens, etwa an einer daneben aufgestellten Papierscala, und lässt nun den Kautschuk von einem Gehülfen electriciren. Der Gehülfe hält zu diesem Zweck in jeder Hand einen isolirten Spitzenkamm, von denen der eine mit der positiven, der andere mit der negativen Electrode einer kräftigen Holtz'schen Maschine in leitender Verbindung steht; zwischen den parallel gehaltenen Kämmen hängt das Kautschukband, dasselbe wird aber nicht von den Spitzen berührt. Indem nun der Gehülfe etwa am obern Ende anfängt und allmählich mit beiden Kämmen herunterfährt, wird ein immer grösserer Theil des Kautschuks electricirt; dem entsprechend beobachtet man eine fortwährende Längenzunahme des Bandes, welche schliesslich, wenn der ganze Streifen electricirt ist, mehrere Centimeter beträgt. Da trockener Kautschuk ein guter Isolator ist, dauert diese Verlängerung längere Zeit. Dieselbe kann aber, wenigstens zum grössern Theil aufgehoben werden, indem man den Streifen entladet, was in ähnlicher Weise geschieht wie das Laden; nur müssen jetzt beide Kämmen zur Erde abgeleitet sein.

Auch Herr Quincke hat (1880) ähnliche Versuche veröffentlicht und glaubt aus denselben schliessen zu dürfen, dass die Elasticität der festen Körper durch electricische Kräfte geändert werde; ich halte eine solche Schlussfolgerung wiederum für sehr gewagt und habe nach einer Prüfung der Quincke'schen Versuche keine Veranlassung gefunden, diese Auffassung zu der meinigen zu machen; da ich jedoch befürchte, dass der vorliegende Aufsatz eine zu grosse Ausdehnung erhalten würde, so möchte ich die Mittheilung der Motive zu meinem ablehnenden Verhalten unterlassen.

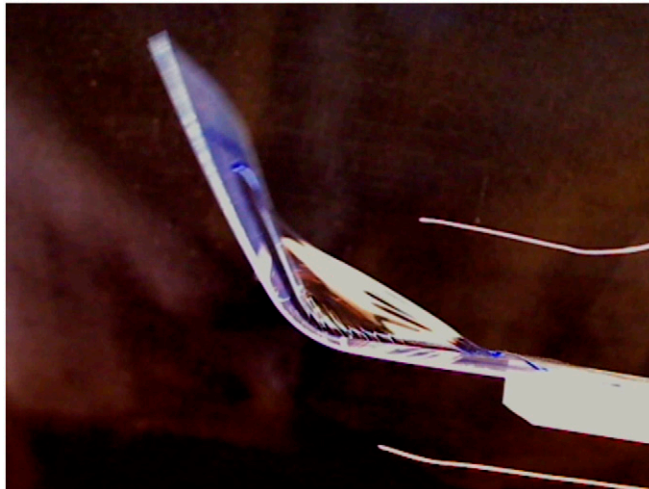
Giessen, September 1880.

Fig. 56. Extracts from Röntgen's original work in German.



Movie S1. Illustration of the reversibility of the large deformations of an elastomer surface with sprayed-on electrical charges.

[Movie S1 \(MPG\)](#)



Movie S2. Illustration of the operation of the electrode-free bending actuator.

[Movie S2 \(MPG\)](#)